Avicenna Journal of Medical Biochemistry
doi:10.34172/ajmb.2020.01 2020 June;8(1):1-14 http://ajmb.umsha.ac.ir

Research Article

Identification of the Anti-sickling Activity of *Anogeissus leiocarpus* and In Silico Investigation of Some of Its Phytochemicals

Taiwo O. Elufioye[1*], Babatunde M. Williams[1], Mojisola C. Cyril-Olutayo[2]

[1]Department of Pharmacognosy, Faculty of Pharmacy, University of Ibadan, Ibadan, Nigeria.
[2]Drug Research and Production Unit, Faculty of Pharmacy, Obafemi Awolowo University, Ile Ife, Nigeria.

*Corresponding author: Taiwo O. Elufioye, Department of Pharmacognosy, Faculty of Pharmacy, University of Ibadan, Ibadan, Nigeria
Email: toonitaiwo@yahoo.com

Received: 15 November 2019
Accepted: 12 March 2020
ePublished: 29 June 2020

Abstract

Background: The anti-sickling activity of *Anogeissus leiocarpus,* a plant used for managing sickle cell disease (SCD), has been previously proven.
Objectives: This study investigated the anti-sickling mechanism of *A. leiocarpus* by probing its effects on Gardos channel (KCNN4), erythropoietin (EPO), erythropoietin receptor (*EPOR*), catalase (CAT), G6pD, D-type cyclins and cyclin-dependent kinase inhibitors (*p21*) gene expression as well as assessing in silico drug-likeness of reported compounds as *EPOR* agonist.
Methods: A total of 18 rats (45-76 g) were selected and divided into 6 groups (n=3). The control group was given water *ad libitum*, standard group was given 0.1 mL/kg of Ciklavit® and experimental group was given daily oral doses of 50-100 mg/kg body weight of crude methanol extract or ethyl acetate fraction (EA-PF). Haematological parameters were analyzed while histopathological and molecular studies of kidney and bone marrow were carried out, followed by RT-PCR analysis of *KCNN4*, *EPO*, *EPOR*, *CAT*, *G6pD*, *p21*, and cyclin-dependent kinase inhibitors. Docking studies of the reported compounds were also done.
Results: EA-PF had an insignificant ($P>0.05$) effect on haematological parameters compared to the basal group. While *CAT* and *p21* acted in a positive feedback loop, *G6pD* was downregulated in the experimental groups. *KCNN4* acted in a negative-feedback mechanism and the upregulation of *EPO* and *EPOR* was followed by increased reticulocytes. Kaempferol, quercetin, and catechin showed non-violation of Lipinski's rule and high binding affinities of 6.5 kcal/mol, 6.7 kcal/mol, and 6.7 kcal/mol, respectively, for EPOR pocket compared to the co-crystallized ligand.
Conclusion: Results suggest that ethyl acetate fraction of *Anogeissus leiocarpus* achieved a steady state level of the Gardos channel and stimulation of EPO expression via EPOR agonist.
Keywords: Sickle cell anaemia, *Anogeissus leiocarpus*, Gardos channel, Erythropoiesis, Mechanism of action

Background

Sickle cell anaemia has emerged as a public health problem with a continued increase in low and middle-income countries especially in sub-Saharan Africa, with Nigeria having the highest number of sickle cell anaemia sufferers in the world (1, 2). The disease is characterized by chronic intravascular haemolysis due to abnormal red blood cells (RBCs) shape that leads to vaso-occlusive crises which is the hallmark of sickle cell disease (SCD) that creates economic burden and makes management difficult in developing countries (3, 4). However, the multifaceted pathophysiology of SCD makes it possible to interrupt the disease at different stages through disruption of the pathology-initiating step of hemoglobin S (HbS) polymerization by inducing higher concentrations of fetal hemoglobin, counteracting endothelial inflammatory and oxidative abnormalities, and improving erythrocyte rehydration (5). Therefore, a multi-target therapeutic approach appears to be most promising.

The biochemical interplay between SS (HbS/HbS) cell dehydration *in vivo* and Gardos channel (a Ca^{2+}-sensitive, intermediate-conductance, K^+-selective channel encoded KCNN4, IK1 or hSK4) has continued to receive considerable research attention. At physiological intracellular Ca^{2+} concentration, Gardos channels are inactive, but it is activated in low-K^+ media and transient increase in Ca^{2+} levels in pathological as well as experimental states was observed. The resulting net loss of KCl and $KHCO_3$ is linked to osmotic-driven water loss that causes cell dehydration referred to as Gardos effect (6-

10). Blockade of the Gardos channel could then have a beneficial effect on the pathophysiology of SCD as a drug target (11-13). Drugs such as charybdotoxin, Clotrimazole® (14), and Senicapoc® (15) have been used as Gardos channel blockers. However, because of the drawbacks of these drugs, which include imperfect selectivity, poor efficacy and attendant toxicity (16), coupled with the fact that more effective therapeutics are required for managing SCD (17,18), the search for new drugs is desirable.

A large number of the world's population resort to plants and traditional medicine for primary health care and the use of plant parts as drug and repositories of pharmacological compounds for drug candidate dates back to prehistoric times (19, 20). Several plants are being used in traditional medicine for the management of sickle cell anaemia and the anti-sickling activity of some of these plants has been scientifically verified. *Cajanus cajan* seeds (21), *Zanthoxylum macrophylla* roots (22, 23), *Parquetina nigrescens* root (24), and *Carica papaya* leaf (25) have been proven to have anti-sickling activity. Some herbal formulations such as Niprisan® (17) and Ajaworon (18) are also commercially available for managing the disease.

Anogeissus leiocarpus is a medicinal plant found in Nigeria's flora with several reported biological activities. Its medicinal values include wound healing (26) as well as treatment for skin diseases, psoriasis, leprosy, diarrhea, fever, rheumatism, and cough (27, 28). The plant has been reported to possess antiproliferative properties against HepG2 hepatocarcinoma cells (29), antitumor activity via angiogenesis pathway (30), as well as antioxidant and antimicrobial activities (30-32). Phytochemical screening identified the presence of flavonoids, terpenoids, tannins, alkaloids, cardiac glycosides, saponins, steroids, anthraquinones, and phenolic compounds in the plant (26, 33).

The in vitro anti-sickling activity of recipe containing *A. leiocarpa* has been previously reported (34). In an earlier study, we also reported the inhibitory and reversal effects of extracts and fractions of the plant on sodium metabisulphite–induced polymerization of sickle cell haemoglobin (35). This study was, therefore, undertaken to elucidate the mechanism of anti-sickling activity of *A. leiocarpus* leaves by investigating its modulation on the basal expression levels of Gardos channel (*KCNN4*), erythropoietin (*EPO*), erythropoietin receptor (*EPOR*), catalase (*CAT*), glucose-6-phosphate dehydrogenase (*G6pD*), cyclin-dependent kinase inhibitor 1 (*p21*) and D-type cyclin (cyclin-D2) in rat model. Molecular docking study was also carried out to estimate the binding affinity of phytochemicals in the plant for EPOR, as a first step in exploring their pro-erythropoietic and hence anti-sickling potencies.

Materials and Methods

Plant Materials

Fresh plant leaves of *Anogeissus leiocarpus* were collected from the Botanical Garden, University of Ibadan, Nigeria. The plant was identified and authenticated by Mr. Oba at the Forest Herbarium Ibadan with the voucher number FHI 109890. The leaves were air-dried, pulverized and extracted with 100% methanol. The extract was filtered and the filtrate was concentrated in vacuo using the rotary evaporator. The methanol extract was fractionated into n-hexane, ethyl acetate, and water.

Drug Ciklavit® was purchased from Mosh Pharmacy, Bodija. Ibadan, Nigeria.

Animals

A total of 18 female albino rats (Swiss strain) weighing between 45-76 g were obtained from the Animal Unit (Centre for Biocomputing and Drug Development, Adekunle Ajasin University, Akungba-Akoko, Ondo State) and divided into six groups (n = 3). The rats were kept under standard laboratory conditions (room temperature range: 22°C-30°C; photoperiod: 12 h light and 12 h dark) all through the period of study and were fed with commercial pelletized broiler finisher feed (produced by Vital Feeds, Ondo, Nigeria) and tap water *ad libitum.* The experimental procedure was conducted according to the International, National and Institutional Guidelines for the Use and Care of Experimental Animals.

Experimental Design

The design of the experiment consisted of negative control group (group 0), which received feed and water *ad libitum*, positive control (group I,) which received 0.1 mL Ciklavit®, the test groups which included group II (50 mg/kg EA-PF), group III (100 mg/kg EA-PF), group IV (50 mg/kg crude extract), and group V (100 mg/kg crude extract). Different doses were administered orally using oropharyngeal cannula once daily for 28 days.

Haematology

At the end of the study, the rats were fasted overnight and anaesthetized with chloroform. Then, blood samples were collected into an EDTA-treated bottle by cardiac puncture for haematological analysis. Haematological analysis was done using Automated Hematologic Analyser (Coulter STKS, Beckman). Packed cell volume (PCV), white blood cell (WBC) count, haemoglobin concentration (HbC), RBC count, mean corpuscular volume (MCV), mean corpuscular haemoglobin (MCH), mean corpuscular haemoglobin concentration (MCHC), neutrophil, lymphocytes, basophil, eosinophil, monocyte, and platelet count were determined.

Histopathology

The kidneys and bone marrows were fixed in 10% formal-

saline, trimmed and embedded in paraffin wax. A manual microtome (Hedee, model no. KD-202C) was used to cut them into thin sections. The sections were subjected to de-paraffinization, rehydration and staining with hematoxylin and eosin (H&E) dyes and mounted for regular histological investigation. The preparations obtained were visualized using a light microscope (Olympus microscope, binocular with camera attached model) at a magnification of ×200.

RNA Isolation

RNA was extracted by the method used by Stead et al (36). The kidney and bone marrow samples were put into separate Eppendorf tubes containing 100 µL RNA snap™ kit reagent (18 mM EDTA, 0.025% sodium dodecyl sulphate, 95% formamide, and 1% 2-mercapto-ethanol) and stored at -70°C until RNA was extracted from them. The tissues were heated on a water-bath for 7 minutes at 95°C and mechanically homogenized. The lysate was centrifuged (LR 56495 Centrifuge Machine ABBOTT) at 16 000 rpm for 30 minutes. The supernatant (containing RNA) was aspirated, treated with 5 µL of 3M sodium acetate (pH 5.2) and 800 µL cold EtOH, and stored for 1 hour at -7°C. Then, it was centrifuged at 16 000 rpm for 30 minutes to form RNA pellets at the bottom and then the supernatant was decanted. RNA pellets were washed twice with 800 µL EtOH (70%) and cooled before re-dissolving in 50 µL nuclease-free water. The concentration was determined by measuring the absorbance at 260 nm (JENWAY 6305 Spectrophotometer) and all samples were diluted to the same concentration.

cDNA Synthesis

Two microliters RTase was added to 20 µL of total RNA and incubated in a thermocycler at 42°C for 1 hour and then at 65°C for 3 minutes for enzyme deactivation. The cDNA was then used as template for PCR amplification.

Reverse Transcription-Polymerase Chain Reaction

Reverse transcription-polymerase chain reaction (RT-PCR) was used to measure relative differences in mRNA levels and normalized against β-actin. Thirty-cycle PCR (MultiGene OptiMax, Labnet International, Inc. Thermocycler) was performed on cDNA template (5 µ) using Taq polymerase Master Mix (10X) (primers specific to different domains with their coding sequence), dNTPs, $MgCl_2$ buffer, reverse and forward primers, and nuclease-free water (5 µL). The specific primers used for rat/mouse β-actin cDNA were as follows: β-actin F5'-ACACTTTCTACAATGAGCTGCG-3', β-actin R5'-ACCAGAGGCATACAGGACAAC-3'; F5'-CCGACCAGGGCATCAAAA-3'; R5'-GAGGCCATAATCCGGATCTTC-3' spanning the *CAT* domain; *G6pD* F5'- GCTATGCCCGTTCCATGCT-3' and R5'- GCGTCCGTCATATCTGCCG-3; *GPX-1* F5'-AGTTCGGACATCAGGAGAATGGCA-3' and R5'-TCACCATTCACCTCGCACTTCTCA-3'; *EPOR*; Cal-channel; *Cyclin-D2*; *p21*, and *EPO*. Each cycle consisted of denaturation at 94°C for 30 seconds, annealing at 55°C for 30 seconds, and extension at 72°C for 30 seconds. A 5-minute pre-denaturation step at 94°C and 5-minute pre-extension step at 72°C were carried out before and after the 30 cycles. The product was loaded into each well of a 0.5% agarose gel for electrophoresis.

Gel Electrophoresis

Amplicons were electrophoresed in 0.5% agarose gel using 0.5x TBE buffer (2.6 g Tris base, 5 g Tris boric acid, and 2 mL 0.5M EDTA), adjusted to pH 8.3 with Sodium hydroxide pellet, stained with 0.5 µL ethidium bromide and visualized as bands by transilluminator. ImageJ was used to crop and analyze the gel images.

Computational Prediction of Ligand Interaction

The X-ray crystal structure of the human EPOR complexed with an antibody (ABT007) was retrieved from the RCSB database and prepared for the docking prediction (37). ABT007 is a highly potent and specific agonistic antibody that interacts with EPOR at an accessible active site made up of Leu26, Trp64, Pro, Glu, 97, 107, His110, Arg111 Val112, and His114. Using ChemBioOffice suite of programs, three-dimensional models were generated for the seven flavonoids, folic acid and the amino acid phenylalanine (L-configuration) (Figure 1). Each compound was energy minimized using the steepest descent algorithm and once minimized, each ligand was saved in the protein databank format. The bound antibody, crystallographic water as well as other crystallographic excipients were removed from the EPOR molecule, after which all missing hydrogen atoms were added using AutoDock tool (38). Using the same docking suite of programs, Gasteiger charges were added to the EPOR molecular structure as well as all nine ligands important in particular for the computation of the electrostatic component of the binding free energies (ΔG). We then constructed a virtual rectangular cuboid, the docking grid, with xyz dimensions sufficiently wide (17Å by 30 Å by 30 Å) to cover all EPOR surface residues defining the epitope employed in interacting with ABT007 as well as the available cavities. Then, AutoDock Vina (39) docking runs were performed for each ligand using a flexible treatment of all torsional degrees of freedom in the ligand molecules while the EPOR structure was kept rigid. For each ligand molecule, the top performing bound ligand conformation was saved and analyzed.

Lipinski's Rule of Five for Drug Likeliness and In Silico ADME Prediction

Six compounds identified in the plant were further evaluated for their drug-like behavior through the analysis of pharmacokinetic parameters required for absorption,

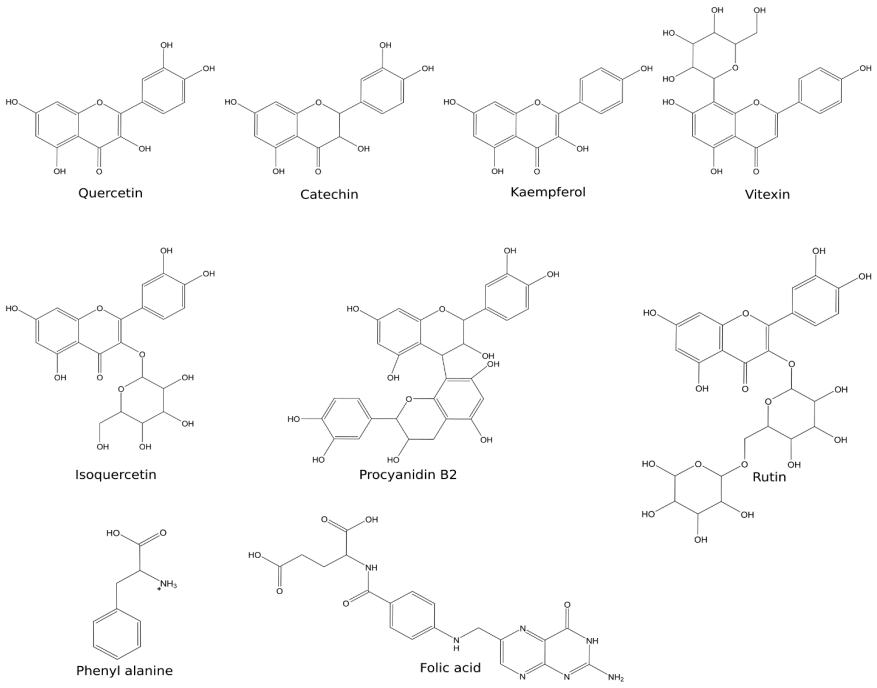

Figure 1. Two Dimensional Structures of the Ligand Molecules Employed for Docking Analysis.

distribution, metabolism and excretion (ADME) using QikProp (40).

Statistical Analysis

Data were expressed as mean ± standard error of mean (SEM). Comparisons were made by one-way (ANOVA) followed by Dunnett's multiple comparisons test using GraphPad Prism version 5.0. $P<0.05$ was considered statistically significant.

Results

The effect of EA-PF and crude extract (CE) was investigated on haematological parameters, and histology of bone marrow and kidney of female Swiss albino rats. These effects were compared with groups that received Ciklavit® (standard drug) and water as placebo (basal control). Moreover, the modulatory effect of the extract and fractions on the expression of genes implicated in SCD was assessed and in silico study of the selected compounds was carried out.

Haematology

The ethyl acetate fraction slightly increased Hb concentration, MCHC, PCV, RBC, and platelet number while the methanol extract at 100 mg/kg increased WBC and all the tested drugs increased MCV. However, these changes in haematological parameters were not significant ($P>0.05$) when compared with groups that reveived Ciklavit® (standard) and water (Figure 2).

Histology of the Bone Marrow

The results of the histological analysis revealed that rats in the basal control group showed high cellularity, normal shapes and sizes (Figure 3A) when compared with cells which assumed different shapes (poikilocytosis) and sizes (anisocytosis) observed in 50 mg/kg b.wt. EA-PF group (Figure 3C). In 100 mg/kg EA-PF group, an abundant number of cells with normal shapes and sizes were observed (Figure 3D). A scanty cellular population with serrated edges was observed in 50 mg/kg CE extract group (Figure 3E) compared to 100 mg/kg CE group, in which cell clumping, small-sized cells and a few abnormally shaped cells were observed (Figure 3F) whereas normally shaped nucleated cells and erythrocytes at the background were seen in Ciklavit® group (Figure 3B).

Histology of the Kidney

Normal histology of rat kidney (glomeruli, tubules, interstitium, and blood vessels) was found in the control group (Figure 4A) hence, no observable lesion. The glomeruli were evenly distributed with and well-packed tufts and tubules were normal with interstitial congestion. At 50 mg/kg, EA-PF-treated group exhibited mild proliferation of mesangial cells in the glomeruli. Moreover, tubules were ectatic and interstitium containing a few cells was observed (Figure 4C). However, no observable lesion was found in kidney of 100 mg/kg EA-PF-treated group (Figure 4D). A dose of 100 mg/kg b.wt. of CE induced atrophy in few of the glomerular tufts and less cellular (Figure 4E). This was supported by tubular epithelial cells which were degenerate and necrotic with prominent casts

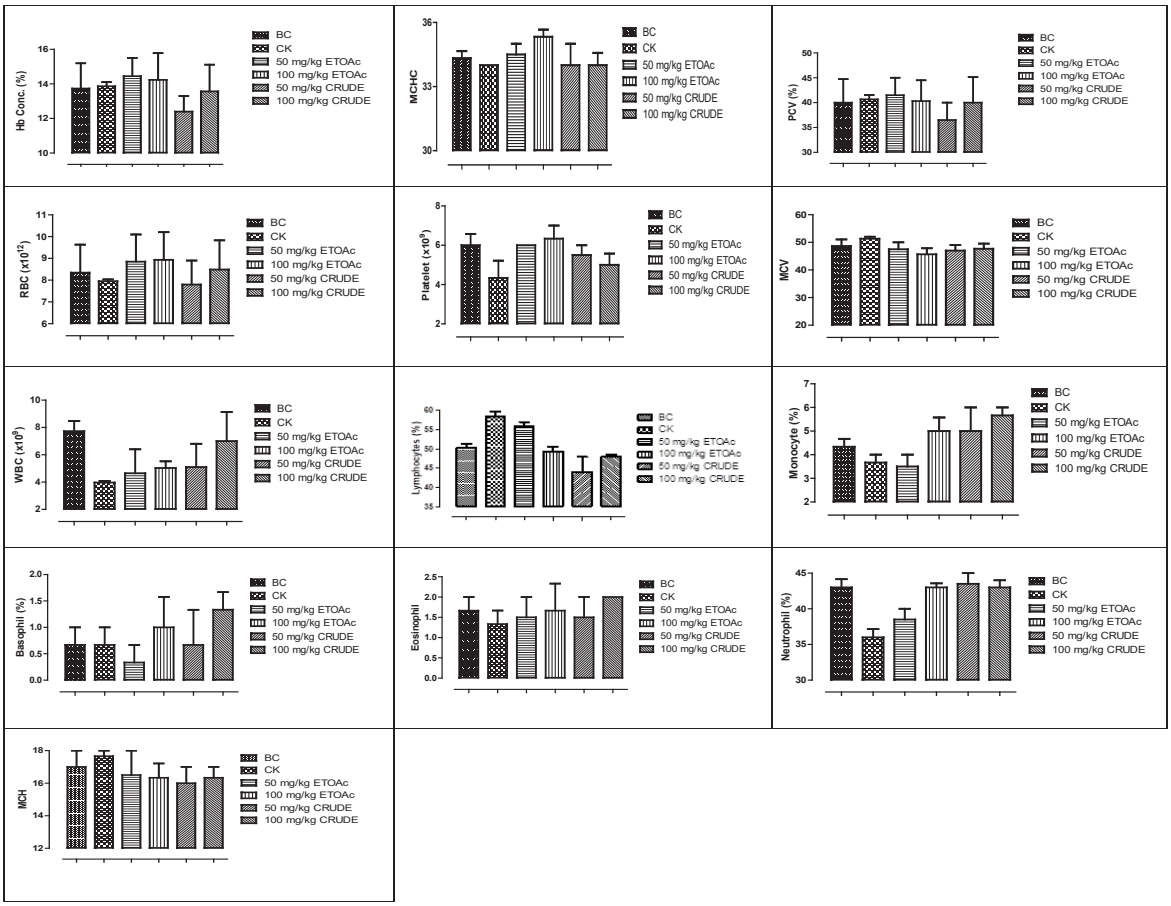

Figure 2. Effect of Ethyl-acetate Partitioned-fraction (EA-PF), Crude Extract (CRUDE) and Ciklavit® (CK) on Haematological Parameters of Nomoxic Female Swiss Albino rats for 28 Consecutive Days.
Data show means ± SEM, n=3. *= $P<0.05$; **= $P<0.001$ relative to basal control (BC).

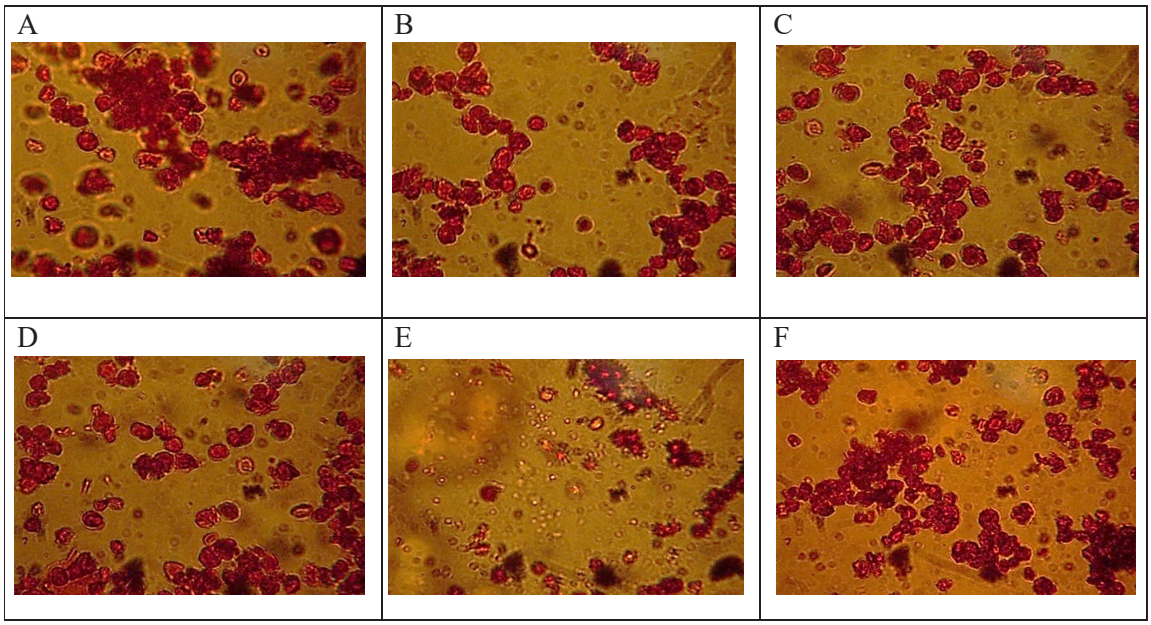

Figure 3. Photomicrographs of Rat Bone Marrows Post-administration of EA-PF, Crude Extract and Ciklavit®, Respectively
(A) Bone Marrow of Rat in the Control Group Received Feed + Water Ad Libitum; (B) Bone Marrow of Rat in Ciklavit® Group Received 0.1 ml/g Ciklavit®; (C and D) Bone Marrows of Rat Received 50 and 100 mg/kg BW EA-PF; (E and F) Bone Marrows of Rat Received 50 and 100 mg/kg BW Crude Extract.

in lumen. There were also a few interstitial cell reactions (Figure 4F). Ciklavit® at the concentration of 0.1 mL/kg b.wt. resulted in a few atrophic glomeruli with accentuated Bowman's space compared to the control group. The tubules were ectatic and the epithelium was attenuated (Figure 4B).

Quantification of mRNA of Specific Genes by RT-PCR and Ethidium Bromide-Stained Agarose Gel Electrophoresis

Agarose gel electrophoresis of reverse transcription-PCR products was used for the detection of specific gene expression profile in the bone marrow and kidney tissues with relative intensities. Lanes 3-6 were obtained from co-exposure to 50 and 100 mg/kg b.wt. of EA-PF and CE while lanes 1 and 2 were basal control and Ciklavit® group, respectively.

KCNN4 expression was modulated in a negative feedback loop in bone marrow (BM) tissues from rat.

$K_{Ca}3.1$ channels are well characterized to promote Ca^{2+} entry by maintaining a driving force and negative membrane potential. To investigate the potential role of KCNN4 (calcium channel) in regulating erythrocyte dehydration, the mRNA expression of *KCNN4* in BM tissues was examined in rats by RT-PCR. It was observed that the 100 mg/kg dose of EA-PF significantly suppressed the expression of *KCNN4* ($P<0.05$) when compared with the other doses. However, the basal control group also showed a significant suppression (Figure 5A).

EPO and EPOR expressions were upregulated in kidney and bone marrow tissues from rat.

To investigate the possible effect of *A. leiocarpus* on EPO and EPOR, mRNA expression of specific genes was quantified by RT-PCR using gel electrophoresis. The relative expression levels of EPO and EPOR transcripts were qualitatively measured and modulation was investigated. It was observed that the EA-PF and the CE produced an increase in cell proliferation of EPOR in a dose-dependent manner with the CE having better effect (Figure 5C). However, the EA-PF at 100 mg/kg significantly increased the expression of EPO (Figure 5B).

CAT, p21, and Cyclin-D2 were transcriptionally upregulated in bone marrow tissues from rat.

Enzyme activity and transcriptional level of *CAT* gene, the main enzyme of antioxidative defence, was upregulated and induced in a dose-dependent manner by all the test drugs. The extract and fractions had better effect than the standard drug (Figure 5D). Downregulation of the expression of cyclin-dependent kinase 1 inhibitor (p21) in bone marrow tissues was observed in response to the 100 mg/kg EA-PF (Figure 5G) while Figure 5H showed that *cyclin D2* was also upregulated dose-dependently.

Downregulation of G6pD expression stimulated antioxidant-switch and cytoprotective effect of G6PD/NADPH/glutathione (GPX-1).

The expression level of Glucose-6-phosphate dehydrogenase (*G6pD*) was higher in response to 100 mg/kg b.wt. EA-

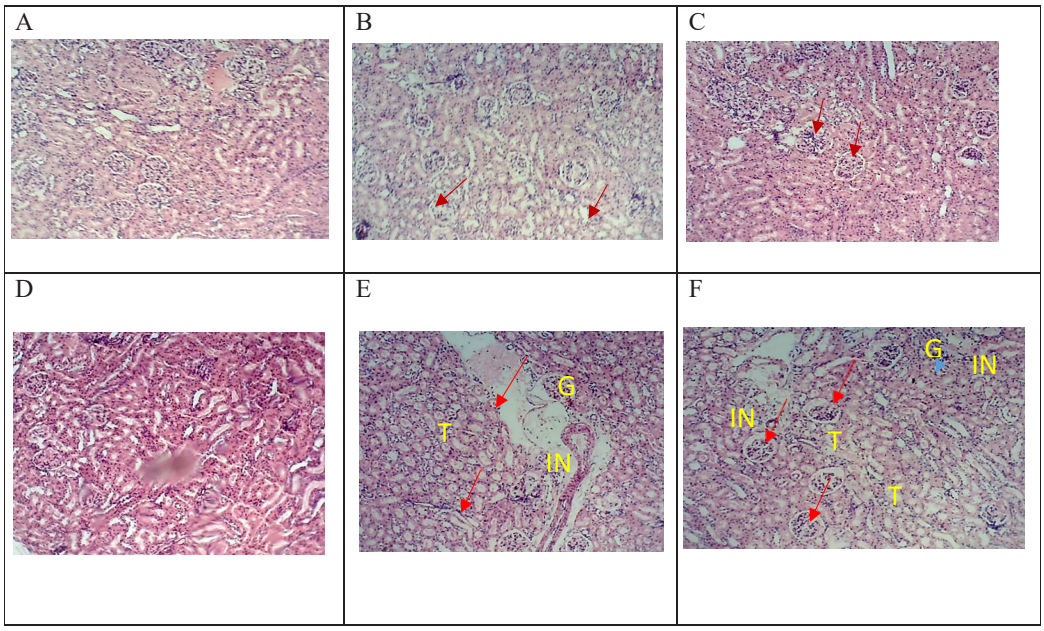

Figure 4. Photomicrographs of Rat Kidneys Post-administration of EA-PF, Crude Extract and Ciklavit®, Respectively (A) Kidney of Rat in the Control Group Received Feed + Water Ad Libitum. (B) Kidney of Rat in Ciklavit® Group Received 0.1 ml/g Ciklavit®; (C and D) Kidney of Rat Received 50 and 100 mg/kg BW EA-PF; (E and F) Kidney of Rat Received 50 and 100 mg/kg BW Crude Extract. T: tubules, G: glomerulus, and IN: interstitium; Hematoxylin and eosin stain, x200.

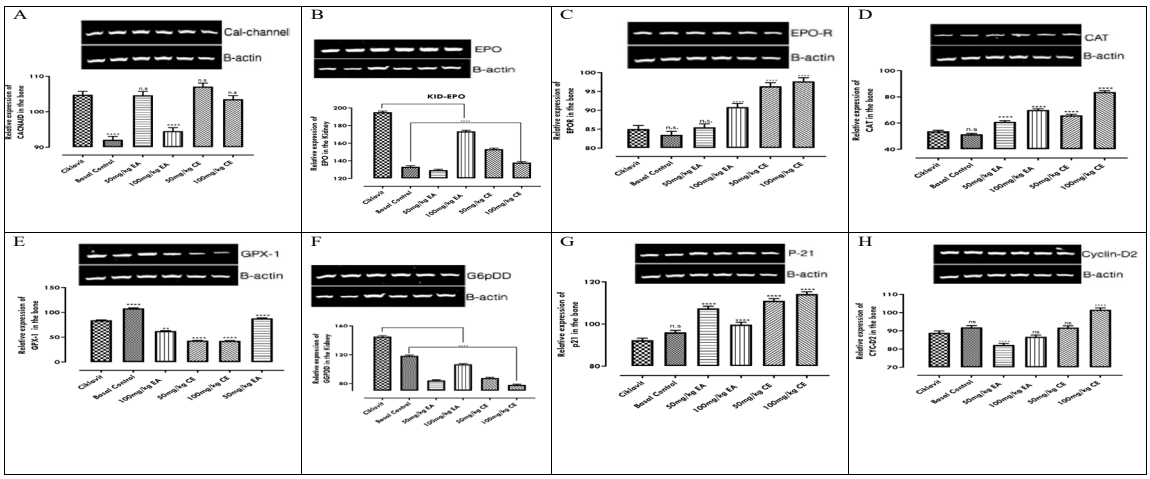

Figure 5. The reverse transcription-PCR gel images are cropped for clarity from the full-length images under the same experimental conditions. Effects of ethyl-acetate partitioned-fraction (EA), crude (CE) and ciklavit on the differential basal level of selected gene expression was compared. Error bars represent standard deviation on the normalized ratio. A Dunnett's multiple comparisons test was performed on the normalized gene expression to check whether the expressions were statistically different between the control and the experimental groups (* = $P<0.05$ versus control; ** = $P<0.001$; n.s = not significant). Amplicons were analysed with agar gel electrophoresis stained with 0.5 µl ethidium bromide of 0.5% agarose gel, o.5x TBE buffer. β-actin (β-ACT) serves as loading control.
Data show means ± S.D, n=3.

PF compared to other test doses which tend to suppress the expression. The standard drug (Ciklavit), however, significantly increased the expression level (Figure 5F).

Ligand-EPOR Interaction

The obtained interaction energy values are presented in Table 1. All seven flavonoids demonstrated moderately strong binding interaction with EPOR even though marginal binding superiority was recorded for quercetin and catechin. Moreover, all flavonoids were slightly better than folic acid (ΔG = -6.3 kcal/mol), this is more so for quercetin (-6.7 kcal/mol), catechin (-6.7 kcal/mol), rutin (-6.6 kcal/mol), and vitexin (-6.6 kcal/mol), whose computed binding free energy values were less than folic acid (0.2 kcal). With L-phenylalanine demonstrating the worst interaction strength with the active site of EPOR, it is very likely that a combination of multiple ring structures and hydrogen-bonding interactions are important for binding at this site. Indeed, a single modification involving the removal of the 3-hydroxyl group in quercetin and kaempferol increased binding by 0.2 kcal. This may suggest the possibility of optimizing the structure of the studied compounds to identify more specific binders.

It is important to note that while multiple cavities were present within the EPOR antibody target surface covered by the employed docking grid, the same cavity was recognized as the best site for ligand interaction by all nine ligands (Figure 6). Binding to this cavity allowed interaction with three important active site residues, Leu26, Arg111, and His114, directly overlooking the binding cavity and in the crystal structure involved in interaction with chain A of the agonistic antibody ABT007 (37). The other active site residues were majorly located in flat areas of EPOR epitope. The binding of the ligands to these shallow regions would come with a high entropic cost related to both desolvation of the ligand molecules and maintenance of an energetically unfavorable bound pose. Within the cavity, however, the bound pose of the ligands was supported by a number of energetically favorable factors including specific electrostatic and hydrogen bonding interactions between Arg111 and His114 of EPOR on one hand and the hydrogen bond donor and acceptor groups of the flavonoids on the other hand (Figure 7). Orienting the hydroxyl groups at 3 position parallel to the plane of the flavonoids ring C (as seen in quercetin and kaempferol) or orthogonal to it (catechin) appears to be trivial for influencing the interaction strength. This perhaps explains why both quercetin and catechin were found to bind to EPOR with equivalent strength. The examination of the

Table 1. The Binding Free Energy Values for Folic Acid, Phenylalanine, and the 7 Studied Flavonoids

Ligand	ΔG (kcal/mol)
Quercetin	-6.7
Catechin	-6.7
Rutin	-6.6
Vitexin	-6.6
Kaempferol	-6.5
Isoquercetin	-6.5
Procyanidin B2 (P-B2)	-6.3
Folic acid	-6.3
Phenylalanine	-4.7
Dehydroquercetin	-6.9
Dehydrokaempferol	-6.9

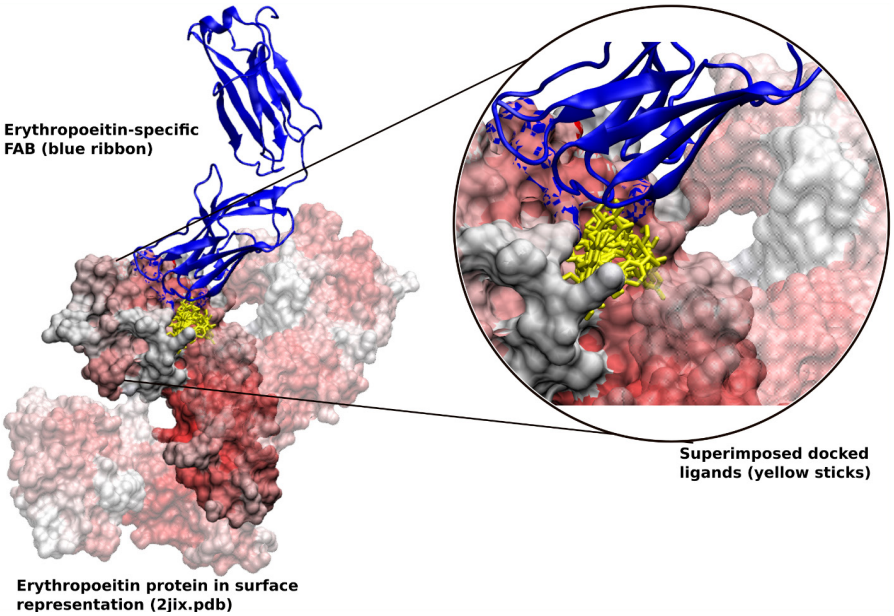

Figure 6. ABT007 (blue ribbon) Interacting with Human EPOR (Surface Representation)
EPOR is colored according to crystallographic thermal fluctuation while EPOR epitope residues involved in binding the antibody ABT007 are shown as blue surface. All nine docked ligands are shown in yellow stick representation superimposed on one another and interacting via a binding cavity that allows hydrogen bond interaction with Arg111. The image was generated using the Visual Molecular Dynamics (85) and the crystallographic structure 2JIX.pdb (37).

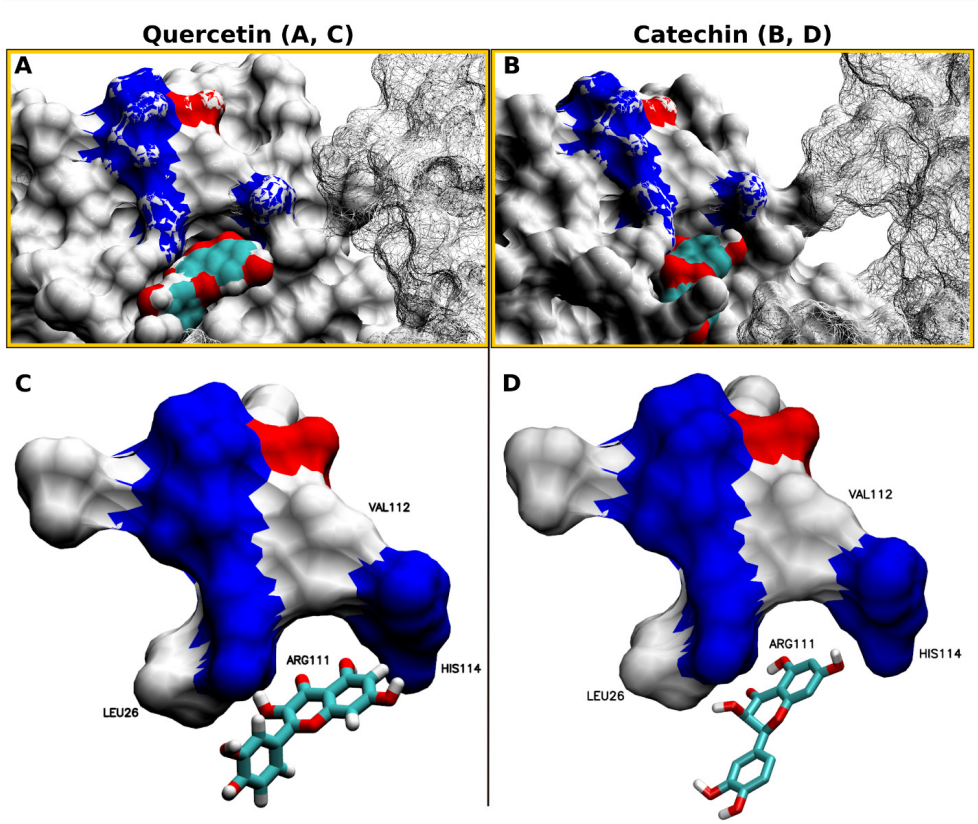

Figure 7. Quercetin (A) and Catechin (B) (surface representation; cyan, red and white depict carbon, oxygen and hydrogen atoms, respectively) Nested Within EPOR Binding Cavity
The epitope-bearing chain C of EPOR is shown in solid white representation while the epitope amino acid residues are shown as blue, red, and white for basic, acidic and hydrophobic amino acids, respectively. Other EPOR chains interacting with its chain C are represented with whitish surface mesh. Figure 7C and D show active site interaction of EPOR Leu26, Arg 111, Val112 and His114 with quercetin and catechin in stick representation, respectively. The image was generated using the Visual Molecular Dynamics (85).

binding interactions as shown in Figure 6 revealed the placement of 3-OH group in flavonoids and the phenyl ring B in the vicinity of the hydrophobic amino acid Leu26 of EPOR. While phenyl ring B in flavonoids appeared optimal for maintaining binding, the 3-OH group seems to be a structural disadvantage. We modified the basic structure of quercetin and kaempferol by removing the 3-OH group and recomputed the binding interaction. In both cases, we recorded a 0.2 kcal/mol improvement in the strength of binding to EPOR. It should, however, be noted that while the approach employed in this work can qualitatively predict the thermodynamic feasibility of an interaction with the epitope region of EPOR that has been recognized as a determinant in agonistic activity of ABT007, a more thorough accounting of the protein dynamical forces (currently beyond the immediate scope of this work) would be necessary for examining the ability of the flavonoids to perturb the structure of EPOR in a fashion conforming to agonistic perturbation of EPOR structure. For this, it would be necessary to perform three groups of multiple independent conformational sampling preferably using enhanced sampling techniques such as the Hamiltonian replica exchange molecular dynamics and Markov state modelling as follows: (*a*) EPOR protein alone, (*b*) EPOR complexed with ABT007, and (*c*) EPOR complexed with the flavonoids. The similarity in the force distribution pattern and the conformational microstates of EPOR obtained with bound ABT007 and flavonoids would be predictive of agonistic tendencies of the latter.

The values are arranged in order of decreasing strength of interaction with the active site of EPOR. The removal of the 3-hydroxy group increased binding affinity of quercetin and kaempferol.

Lipinski's Rule, ADME Descriptor and Toxicity Screening

Three flavonoids, quercetin, catechin, and kaempferol as well as folic acid were analyzed based on Lipinski's rule of five and further subjected to ADME analysis using the Qikprop tool.

The predicted values according to Lipinski's rule are as reported in Table 2 for both the hit compounds and folic acid. The hit compounds appeared to have performed better than folic acid on a number of specified parameters.

For intestinal absorption, quercetin and catechin showed relatively lower passive absorption (63% and 66%) compared to kaempferol (79% absorption) (Table 3). A P_{Caco-2} (nm/sec) (Caco-2 cell permeability) of 9.57744 shows a moderate permeability (4~70) for kaempferol.

The toxicity of the three most promising hit compounds was predicted using preADMET server. The Ames test was used to predict mutagenicity while mouse and rat models were used to predict carcinogenicity (Table 4).

Discussion

SCD is a general term that refers to both homozygous sickle cell anemia and heterozygous SCD. It is the most common genetic disorder caused by inheriting point mutations that change glutamic acid (Glu6) to valine (Val6) in the β chain of hemoglobin. On the basis of the current understanding of the molecular pathogenesis of SCD, a few independent treatment approaches have been proposed (41). These approaches include the use of agents that modify rheological properties of the blood, prevent dehydration of the hemoglobin, exhibit covalent binding to hemoglobin, increase the expression of gamma globin and fetal hemoglobin, increase the bioavailability of nitric

Table 2. Lipinski's Rule of 5 Parameters for Quercetin, Catechin and Kaempferol, and Folic Acid

Ligand	HBD[j]	HBA[j]	MW[k]	QPlogPo/w[l]	Rot B[m]	TPSA[n]	QLogBB[o]	CNS[p]	RO5[q]
Kaempferol	4	6	286.24	1.024	1	107	-1.81	-2	0
Quercetin	5	7	302.24	0.349	1	127	-2.332	-2	0
Catechin	5	6	290.272	0.422	1	110	-1.941	-2	0
Folic acid	6	10	441.404	-2.81	9	209.8	-4.753	-2	2

Molecular Descriptors of the Lead Hit Compounds: [i] Number of hydrogen-bonds donors ≤ 5; [j] number of hydrogen-bonds acceptors ≤ 10; [k] molecular weight < 500; [l] predicted octanol/water partition < 5; [m] number of rotatable bond (0-15), a topological parameter as a measure of molecular flexibility for oral drug bioavailability; [n] (A^2) topological polar surface area, a chemical descriptor for passive molecular transport through membranes

Table 3. Absorption Properties of Quercetin, Catechin, and Kaempferol Using QikProp Module (40)

Ligand	Absorption							
	HIA[a] (%)	QPP_{CaCO2}[b]	P_{MDCK}[c]	P_{skin}[d]	QPLogS[e]	#metab[f]	QPLoghERG[g]	RO3[h]
Kaempferol	79.439289	55.946	0.286076	-4.32558	-3.021	4	-5.03	0
Quercetin	63.485215	19.683	0.172765	-4.43341	-2.782	5	-4.943	1
Catechin	66.707957	50.337	0.394913	-4.29301	-2.653	7	-4.862	1

Molecular Descriptors of the Lead Hit Compounds: [a] percentage of human intestinal absorption (<25% poor, > 80% high); [b] predicted apparent Caco-2 cell permeability (PCaco > 22 nm/s); [c] Maden Darby Canine Kidney cell permeability in nm/s (<25 poor, > 500 high); [d] skin permeability; [e] (> -5.7): predicted aqueous solubility (-6.5 – 0.5); [f] number of likely metabolic reactions (1-8); [g] predicted IC_{50} value for blockage of hERG K^+ channels (acceptable range: above –5.0); [h] Jorgensen's rule of three (maximum is 3).

Table 4 . The Results of Mutagenicity (Ames test) and Carcinogenicity (Mouse and Rat) of Ligands Calculated Using PreADMET Server

Ligand	Ames test (Mutagenicity)	Carcinogenicity	
		Mouse	Rat
Kaempferol	Mutagenic	Negative	Positive
Quercetin	Mutagenic	Negative	Positive
Catechin	Mutagenic	Negative	Negative

oxide and reduce iron overload (42). Others are stem cell transplantation, which is the only cure to date, and gene therapy (43).

In a previous study, we established the inhibitory and reversal effects of *A. leiocarpa* on sodium metabisulphite–induced polymerization of sickle cell haemoglobin (35). In a further attempt to explore the possible use of this plant in the management of SCD, this research was carried out to unfold the mechanism of its anti-sickling effect by analyzing the effects of extract and the most active fractions from the plant on hematological parameters, *KCNN4*, EPO (kidney), EPOR (bone marrow), *CAT*, *G6pD*, D-type cyclins (*cyclin D2*), and cyclin-dependent kinase inhibitors (*p21*) expression. In silico drug-likeness of some compounds already reported in the plant was also assessed as *EPOR* agonist.

The assessment of hematological parameters is one simple and convenient way of evaluating the effectiveness of a therapy in blood disorders such as SCD (44, 45). Hematological parameters such as MCH, red cell distribution width, and reticulocyte counts are important in the diagnosis, treatment and monitoring of SCD (44, 46). Leukocytes are readily accessible cell population and they are involved in SCD vasculopathy (47). The levels of MCH, WBC, basophil, eosinophils, neutrophils, lymphocytes, and monocytes were determined in response to Ciklavit and different extracts of *A. leiocarpa*. As observed, the methanol CE and ethyl acetate partitioned fraction of *A. leiocarpus* did not cause significant ($P > 0.05$) change in hematological parameters when compared to the basal control group (Figure 2). This finding corroborates the results obtained by Agaie et al and Chidozie et al (48, 49) whose studies revealed that significant hematological changes were not observed in extract treated groups when compared to the control. However, it was agreed that *A. leiocarpus* possess potent pro-hematological agents capable of normalizing biochemical abnormalities associated with blood disorders (48, 49). Meanwhile, Sarkiyayi and Aileru (50) reported that methanol extract of the plant exhibited a dose-dependent increase in certain hematological parameters such as RBC count, platelet count, and MCH. Cells from the bone marrow were examined for the possible effect of the extract on the RBCs. There was an observable increase in the cellularity with normal shapes and sizes in the bone marrow of the animals treated with 100 mg/kg of both EA-PF and CE, which is comparable to the positive control (Figure 3A-F). Therefore, *A. leiocarpus* appeared to improve the number and quality of RBCs in the treated groups.

The *KCNN4*, also known as Gardos channel gene and found in human erythrocytes, is a gene encoding $K_{Ca}3.1$ protein which is a part of the voltage-independent potassium channel activated by intracellular calcium. This channel is considered important in SCD because it is the major pathway for cell shrinkage via KCl and water loss that occurs in SCD (51). In this study, we observed that the expression of *KCNN4* was suppressed in response to 100 mg/kg EA-PF (Figure 5A). This suggests that since K^+ efflux through the Gardos channel of human RBCs would be obstructed and Ca^{+2} import through the calcium-release activated calcium channel reduced, leading to the prevention of Gardos channel activation in RBCs to prevent dehydration in SCD (Figure 5A). This indicates one possible mechanism of action of the extracts of *A. leiocarpus*

EPO, also called hematopoietin or haemopoietin, is a hormone produced primarily by the kidneys and is responsible for controlling the production of RBC by regulating the differentiation and proliferation of erythroid progenitor cells in the bone marrow. Previous studies have reported low level of EPO in patients with SCD (52). However, patients with SCD who are not in crisis have high level of EPO but it is generally lower compared to healthy patients with chronic anaemia (53). EPO is also used in the management of SCD (54).

In this study, *A. leiocarpus* had a significant ($P < 0.05$) up-regulation effect on EPO with the best effect observed in the 100 mg/kg EA-PF (Figure 5B) as well as EPOR in bone marrow with CE at 100 mg/kg having the best effect (Figure 5C). One possible mechanism by which ethyl acetate fraction of *A. leiocarpus* may stimulate erythropoiesis is by decreasing the rate of oxidant-induced hemolysis due to the presence of antioxidants flavonoids in the plant (55). This antioxidant mechanism will usually prolong the average life span of individual RBCs. *A. leiocarpus* have been reported to contain high flavonoid content (31, 33, 56) and flavonoids in *A. leiocarpus* have been identified as responsible for the scavenging or chelating activity against oxidative stress (26, 57). Different researches have shown that the expression of EPO can be modulated by flavonoids. Esomonu et al (58) and Oluyemi et al (59) reported increased erythropoiesis in rat models received flavonoids extract of *Garcinia kola* while Zheng et al (60) reported that flavonoids of *Radix astragali* stimulated the expression of EPO in cultured human embryonic kidney fibroblasts.

Oxidative stress has been associated with the pathophysiology of several diseases including SCD. Oxidation reactions produce reactive oxygen species (ROS) which can start chain reactions capable of damaging cells of the body. Therefore, oxidative stress, which occurs in sickle

cell patients due to the constant release of ROS, can result in endothelial dysfunction and acute inflammation (61). Antioxidants, which include some vitamins (C and E) as well as certain enzymes such as CAT, superoxide dismutase (*SOD*), and peroxidases, are involved in terminating the chain reaction generated by ROS, thus playing a protective role (61, 62). From our studies, there was an upregulation of *CAT* transcription in a dose-dependent manner in the BM of animals received different doses of the extract and fraction of *A. leiocarpus* (Figure 5D). Both the ethyl acetate fraction and the methanol extract had a significant effect compared to the basal and positive control groups. This then suggests the possible protection of RBCs from the deleterious effects of ROS in sickle cell anemia. This activity can also be attributed to the presence of flavonoids in the plant. Flavonoids are known to regulate the expression of many genes (63). Specifically, the upregulation of the expression of *CAT* has been attributed the certain flavonoids like curcumin (64).

Various researchers have suggested different associations between SCD and *G6pD*. They include no correlation (65, 66), damaging (67,68), and beneficial (69, 70) effects. Therefore, our study also evaluated the effect of the extracts on *G6pD* gene expression. There was a significant increase in the expression of the *G6pD* gene in the animals treated with 100 mg/kg EA-PF when compared with other doses (Figure 5F). However, this increase may have no implication as previous research has reported no significant difference in hematological parameters, incidence of painful episodes, anemia episodes, sepsis or severity of hemolysis in patients with or without *G6pD* deficiency (5, 14)

Cyclins are components of the core cell cycle machinery involved in cell cycle progression. They form holoenzymes and activate cyclin-dependent protein kinases (Cdk) (71). *Cyclin D* is one of the most important cyclins and it connects with four Cyclin-dependent kinases (Cdks 2, 4, 5, and 6) (72). Through activation of CDK4 and CDK6, D-type cyclins accelerate G_0/G_1 to S-phase transition and mediate mitogenic signals, including those signaled through cytokine receptors (73). We observed a dose-dependent increase in *cyclin D2* expression in the treated groups (Figure 5H). Enhanced *cyclin D2* expression could potentially promote proliferation of hematopoietic stem and progenitor cells (74, 75). This could explain the pro-hematological tendency of *A. leiocarpus* as reported by previous studies (48, 49). However, cyclin-dependent kinase inhibitors (CKIs) inhibit cell division by antagonizing the activities of specific Cdks. CKIs include *p21* and *p27* which are potent inhibitors of CDK2 that is responsible for the regulation of hematopoietic proliferation (76). The ability of *p21* to promote cell cycle inhibition positively correlates with the suppression of genes that are important for cell cycle progression (77). Therefore, downregulation of the gene encoding *p21* would be of advantage in the management of SCD. Our study showed a higher expression of *p21* gene in the treated groups when compared with both the positive and basal control groups (Figure 5G). This indicates that the plant probably does not work through this mechanism of downregulating cyclin-dependent kinase inhibitors.

Protein-ligand molecular interaction plays a significant role in structure-based drug design by predicting the binding conformation or pose of the ligand bound to the protein, and this can be quantified based on the shape and electrostatic interaction between the ligand and protein (78). The totality of interaction observed is approximated to be the docking score of the ligand into the binding pocket of the protein (78). Docking score is expressed in negative value of energy in Kcal/mol where the lower the negative total energy (E), the stronger the interaction between the ligands and the protein (79). Therefore, docking experiments predict the best binding conformation of compounds at the binding pocket of the protein and the interaction between the ligand and the residues at the active site of the protein. In silico study was carried out to predict pro-erythropoietic activity of the hit compounds through molecular docking. The mechanism of interaction of potential stimulation of the EPOR is dependent on the formation of different types of bonds between the amino acid residues at the active site and the ligand. The library of compounds generated was subjected to docking experiment to determine those with high binding energy. The docking result showed good binding energy against EPOR for three compounds (quercetin, kaempferol, and catechin) of *A. leiocarpus* out of the six compounds retrieved from NCBI database and screened. The docking results and ADME screening of the phyto-chemical and co-crystallized ligands are shown in Tables 1 and 4. Quercetin, kaempferol, and catechin produced better scoring results than folic acid, thus implying a high *EPOR* binding affinity. Codorniu-Hernández et al (80) carried out docking studies to understand flavonoid–protein interactions. The results indicated that hydrophilic amino acid residues demonstrated high-affinity interactions with flavonoids, as it was predicted by the theoretical affinity order. The docking modes among catechin molecules and four proteins (human serum albumin, transthyretin, elastase, and renin) also give credence to this finding (81).

Physically significant descriptors and pharmaceutically relevant properties of compounds among which were molecular weight, log p, H-bond donors, and H-bond acceptors according to the Lipinski's rule of five (82), which is a rule of thumb to evaluate drug-likeness or determine if a chemical compound with a certain pharmacological or biological activity has properties that would make it a likely orally active drug in humans. The rule describes molecular properties important for drug pharmacokinetics in the human body, including its ADME. The in silico protein target studies and ADME toxicity analysis revealed that Kaempferol, quercetin, and catechin presented good

absorption parameters and potentials to permeate the blood brain barrier with less biological risk in mouse compared to rat (Table 4). Additionally, the predicted IC_{50} values for quercetin and catechin were within an acceptable range. Kaempferol and quercetin were consistent with Jorgensen's "rule of three": log S > –6, PCaco > 30 nm/s, and maximum number of primary metabolites of 6 (Table 4) (83). It is known that glycosylation of flavonoids increases solubility in the aqueous cellular environment and protects the reactive hydroxyl groups from auto-oxidation (84), as the most reactive hydroxyl groups (7-OH in flavones or the 3-OH in flavonols) in flavonoids are generally glycosylated. This also explains why kaempferol and quercetin are more likely to be orally available with a high drug-likeness property.

Conclusion

Anogeissus leiocarpus leaves showed effects on both EPO and EPORs in female Swiss albino rats, with a potential to reverse pathologic dehydration of red cells under sickling conditions. The upregulation of EPO and negative feedback mechanism of the calcium channel in the experimental models proves its potency as both a pro-erythropoietic agent and a Gardos channel blocker. Extracts from the plant also enhanced *cyclin D2* expression and thus could potentially promote the proliferation of hematopoietic stem cells. It also upregulated *CAT* gene expression suggesting that it can protect RBCs from the damaging effects of ROS experienced in sickle cell anemia. The strong ligand-receptor binding complex structure predicted from computational method was consistent with the upregulation of *EPOR* and *EPO* expression, thus contributing to erythropoiesis stimulation. Compounds in the plant also satisfied the Lipinski's rule of five with zero violations suggesting that these phytochemicals portend to be orally active compounds that may be useful in managing SCD.

Authors' Contributions

TOE designed the experiments, supervised the work, interpreted the data and produced the final manuscript. BMW carried out the experimental work, analyzed the data and wrote the draft manuscript. MCC Co-supervised the work and analyzed the data and edited the manuscript.

Conflict of Interest Disclosures

Authors declare no conflict of interests.

Ethical Issues

The experimental procedure was conducted according to the International, National and Institutional Guidelines for the Use and Care of Experimental Animals.

Acknowledgements

The authors would like to express their gratitude to Dr. I.O Omotuyi from the Centre for Biocomputing and Drug Development, Adekunle Ajasin University, Akungba-Akoko.

References

1. Piel FB, Hay SI, Gupta S, Weatherall DJ, Williams TN. Global burden of sickle cell anaemia in children under five, 2010-2050: modelling based on demographics, excess mortality, and interventions. PLoS Med. 2013;10(7):e1001484. doi: 10.1371/journal.pmed.1001484.
2. Obinna C. Pain and Penury of Sickle Cell Disease not Beyond Science. WHO; 2012.
3. Amer J, Ghoti H, Rachmilewitz E, Koren A, Levin C, Fibach E. Red blood cells, platelets and polymorphonuclear neutrophils of patients with sickle cell disease exhibit oxidative stress that can be ameliorated by antioxidants. Br J Haematol. 2006;132(1):108-13. doi: 10.1111/j.1365-2141.2005.05834.x.
4. Kauf TL, Coates TD, Huazhi L, Mody-Patel N, Hartzema AG. The cost of health care for children and adults with sickle cell disease. Am J Hematol. 2009;84(6):323-7. doi: 10.1002/ajh.21408.
5. Steinberg MH. Pathophysiologically based drug treatment of sickle cell disease. Trends Pharmacol Sci. 2006;27(4):204-10. doi: 10.1016/j.tips.2006.02.007.
6. Ataga KI, Reid M, Ballas SK, Yasin Z, Bigelow C, James LS, et al. Improvements in haemolysis and indicators of erythrocyte survival do not correlate with acute vaso-occlusive crises in patients with sickle cell disease: a phase III randomized, placebo-controlled, double-blind study of the Gardos channel blocker senicapoc (ICA-17043). Br J Haematol. 2011;153(1):92-104. doi: 10.1111/j.1365-2141.2010.08520.x.
7. Thompson-Vest N, Shimizu Y, Hunne B, Furness JB. The distribution of intermediate-conductance, calcium-activated, potassium (IK) channels in epithelial cells. J Anat. 2006;208(2):219-29. doi: 10.1111/j.1469-7580.2006.00515.x.
8. von Hahn T, Thiele I, Zingaro L, Hamm K, Garcia-Alzamora M, Kottgen M, et al. Characterisation of the rat SK4/IK1 K(+) channel. Cell Physiol Biochem. 2001;11(4):219-30. doi: 10.1159/000051936.
9. Rhoda MD, Apovo M, Beuzard Y, Giraud F. Ca2+ permeability in deoxygenated sickle cells. Blood. 1990;75(12):2453-8.
10. Gardos G. The function of calcium in the potassium permeability of human erythrocytes. Biochim Biophys Acta. 1958;30(3):653-4. doi: 10.1016/0006-3002(58)90124-0.
11. Wulff H, Castle NA. Therapeutic potential of KCa3.1 blockers: recent advances and promising trends. Expert Rev Clin Pharmacol. 2010;3(3):385-96. doi: 10.1586/ecp.10.11.
12. Faber ES, Sah P. Calcium-activated potassium channels: multiple contributions to neuronal function. Neuroscientist. 2003;9(3):181-94. doi: 10.1177/1073858403009003011.
13. Brugnara C, Gee B, Armsby CC, Kurth S, Sakamoto M, Rifai N, et al. Therapy with oral clotrimazole induces inhibition of the Gardos channel and reduction of erythrocyte dehydration in patients with sickle cell disease. J Clin Invest. 1996;97(5):1227-34. doi: 10.1172/jci118537.
14. Steinberg MH, Brugnara C. Pathophysiological-based approaches to treatment of sickle cell disease. Annu Rev Med. 2003;54:89-112. doi: 10.1146/annurev.med.54.101601.152439.
15. Stocker JW, De Franceschi L, McNaughton-Smith GA, Corrocher R, Beuzard Y, Brugnara C. ICA-17043, a novel Gardos channel blocker, prevents sickled red blood cell dehydration in vitro and in vivo in SAD mice. Blood. 2003;101(6):2412-8. doi: 10.1182/blood-2002-05-1433.
16. Gee BE. Biologic complexity in sickle cell disease: implications

for developing targeted therapeutics. ScientificWorldJournal. 2013;2013:694146. doi: 10.1155/2013/694146.
17. Iyamu EW, Turner EA, Asakura T. Niprisan (Nix-0699) improves the survival rates of transgenic sickle cell mice under acute severe hypoxic conditions. Br J Haematol. 2003;122(6):1001-8. doi: 10.1046/j.1365-2141.2003.04536.x.
18. Moody JO, Ojo OO, Omotade OO, Adeyemo AA, Olumese PE, Ogundipe OO. Anti-sickling potential of a Nigerian herbal formula (ajawaron HF) and the major plant component (*Cissus populnea* L. CPK). Phytother Res. 2003;17(10):1173-6. doi: 10.1002/ptr.1323.
19. World Health Organization (WHO). WHO Traditional Medicine Strategy: 2014-2023. Geneva: WHO; 2013.
20. Mbula JP, Kwembe JTK, Tshilanda DD, Ngobua KN, Kabena ON, Nsimba SM, et al. Antisickling, antihemolytic and radical scavenging activities of essential oil from *Entandrophragma cylindricum* (Sprague) Sprague (Meliaceae). J Adv Med Life Sci. 2018;6(2):1-5. doi: 10.5281/zenodo.1167931.
21. Ekeke GI, Shode FO. Phenylalanine is the predominant antisickling agent in Cajanus cajan seed extract. Planta Med. 1990;56(1):41-3. doi: 10.1055/s-2006-960880.
22. Sofowora EA, Isaac-Sodeye WA, Ogunkoya LO. Isolation and characterisation of an antisickling agent from *Fagara zanthoxyloides* root. Lloydia. 1975;38(2):169-71.
23. Elekwa I, Monanu MO, Anosike EO. In vitro effects of aqueous extracts of *Zanthoxylum macrophylla* roots on adenosines triphosphatases from human erythrocytes of different genotypes. Biokemistri. 2005;17(1):19-25. doi: 10.4314/biokem.v17i1.32584.
24. Kade IJ, Kotila OO, Ayeleso AO, Olaleye AA, Olawoye TL. Antisickling properties of *Parquetina nigrescens*. Biomed Res. 2003;14:185-8.
25. Imaga NOA, Gbenle GO, Okochi VI, Akanbi SO, Edeoghon SO, Oigbochie V, et al. Antisickling property of Carica papaya leaf extract. Afr J Biochem Res. 2009;3(4):102-6.
26. Barku VY, Boye A, Ayaba S. Phytochemical screening and assessment of wound healing activity of the leaves of Anogeissus leiocarpus. Eur J Exp Biol. 2013;3(4):18-25.
27. Okpekon T, Yolou S, Gleye C, Roblot F, Loiseau P, Bories C, et al. Antiparasitic activities of medicinal plants used in Ivory Coast. J Ethnopharmacol. 2004;90(1):91-7. doi: 10.1016/j.jep.2003.09.029.
28. Singh D, Baghel US, Gautam A, Baghel DS, Yadav D, Malik J, et al. The genus *Anogeissus*: a review on ethnopharmacology, phytochemistry and pharmacology. J Ethnopharmacol. 2016;194:30-56. doi: 10.1016/j.jep.2016.08.025.
29. Olugbami JO, Damoiseaux R, France B, Onibiyo EM, Gbadegesin MA, Sharma S, et al. A comparative assessment of antiproliferative properties of resveratrol and ethanol leaf extract of *Anogeissus leiocarpus* (DC) Guill and Perr against HepG2 hepatocarcinoma cells. BMC Complement Altern Med. 2017;17(1):381. doi: 10.1186/s12906-017-1873-2.
30. Hassan LEA, Al-Suede FS, Fadul SM, Abdul Majid AMS. Evaluation of antioxidant, antiangiogenic and antitumor properties of *Anogeissus leiocarpus* against colon cancer. Angiotherapy. 2018;1(2):56-66.
31. Elufioye TO, Olaifa OA. Comparison of the antioxidant activity with the total phenolic and total flavonoid contents of the leaves and stem-bark of *Anogeissus leiocarpa* (DC.) Guill & Pirr. (Combretaceae). Niger J Pharm Sci. 2016;12(2):71-81.
32. Konaté K, Kiendrébéogo M, Ouattara MB, Souza A, Lamien-Meda A, Nongasida Y, et al. Antibacterial potential of aqueous acetone extracts from five medicinal plants used traditionally to treat infectious diseases in Burkina Faso. Curr Res J Biol Sci. 2011;3(5):435-42.
33. Edewor TI, Akpor OB, Owa SO. Determination of antibacterial activity, total phenolic, flavonoid and saponin contents in leaves of *Anogeissus leiocarpus* (DC.) Guill and Perr. J Coast Life Med. 2016;4(4):310-4. doi: 10.12980/jclm.4.2016J5-218.
34. Egunyomi A, Moody JO, Eletu OM. Antisickling activities of two ethnomedicinal plant recipes used for the management of sickle cell anaemia in Ibadan, Nigeria. Afr J Biotechnol. 2009;8(1):20-5.
35. Elufioye TO, Olaifa OA, Cyril-Olutayo MC. Inhibitory and reversal effects of extracts and fractions of *Anogeissus leiocarpa* (DC.) Guill. & Perr. on sodium metabisulphite–induced polymerization of sickle cell haemoglobin Curr Tradit Med. 2019;5(3):257-67. doi: 10.2174/2215083805666190412162414.
36. Stead MB, Agrawal A, Bowden KE, Nasir R, Mohanty BK, Meagher RB, et al. RNAsnap: a rapid, quantitative and inexpensive, method for isolating total RNA from bacteria. Nucleic Acids Res. 2012;40(20):e156. doi: 10.1093/nar/gks680.
37. Liu Z, Stoll VS, Devries PJ, Jakob CG, Xie N, Simmer RL, et al. A potent erythropoietin-mimicking human antibody interacts through a novel binding site. Blood. 2007;110(7):2408-13. doi: 10.1182/blood-2007-04-083998.
38. Morris GM, Huey R, Lindstrom W, Sanner MF, Belew RK, Goodsell DS, et al. AutoDock4 and AutoDockTools4: automated docking with selective receptor flexibility. J Comput Chem. 2009;30(16):2785-91. doi: 10.1002/jcc.21256.
39. Trott O, Olson AJ. AutoDock Vina: improving the speed and accuracy of docking with a new scoring function, efficient optimization, and multithreading. J Comput Chem. 2010;31(2):455-61. doi: 10.1002/jcc.21334.
40. Schrödinger S. Release 2018-1: QikProp, LLC. New York, NY: 2018.
41. Bunn HF. Pathogenesis and treatment of sickle cell disease. N Engl J Med. 1997;337(11):762-9. doi: 10.1056/nejm199709113371107.
42. de Melo TR, dos Reis Ercolin L, Chelucci RC, Melchior AC, Lanaro C, Chin CM, et al. Sickle Cell Disease–Current Treatment and New Therapeutical Approaches. In: Minshi A, ed. Inherited Hemoglobin Disorders. InTech Open; 2015. doi: 10.5772/60515.
43. Gardner RV. Sickle cell disease: advances in treatment. Ochsner J. 2018;18(4):377-89. doi: 10.31486/toj.18.0076.
44. Yenilmez ED, Tuli A. Laboratory Approach to Anemia. In: Current Topics in Anemia. Intech Open; 2017. doi: 10.5772/intechopen.70359.
45. Dong M, Mizuno T, Vinks AA. Opportunities for model-based precision dosing in the treatment of sickle cell anemia. Blood Cells Mol Dis. 2017;67:143-7. doi: 10.1016/j.bcmd.2017.08.007.
46. Hanna J, Wernig M, Markoulaki S, Sun CW, Meissner A, Cassady JP, et al. Treatment of sickle cell anemia mouse model with iPS cells generated from autologous skin. Science. 2007;318(5858):1920-3. doi: 10.1126/science.1152092.
47. Jison ML, Munson PJ, Barb JJ, Suffredini AF, Talwar S, Logun C, et al. Blood mononuclear cell gene expression profiles characterize the oxidant, hemolytic, and inflammatory stress of sickle cell disease. Blood. 2004;104(1):270-80. doi: 10.1182/blood-2003-08-2760.
48. Agaie BM, Onyeyili PA, Muhammad BY, Ladan MJ. Some toxic effects of aqueous leaf extract of Anogeissus leiocarpus in rats. J Pharmacol Toxicol. 2007;2(4):396-401. doi: 10.3923/jpt.2007.396.401.
49. Chidozie VN, Adoga GI. Toxicological effects of aqueous extract of *Anogeissus leiocarpus* leaf, *Carica papaya* leaf, and *Mangifera indica* stem bark (a herbal product used against typhoid fever) on Albino rats. Cancer Biol. 2014;4(4):26-34.
50. Sarkiyayi S, Aileru AE. Phytochemical screening and hematological studies of the leaves of *Anogeissus leiocarpus* on gentamicin induced rats. Bagale J Pure Appl Sci. 2016;10(1):123-41.

51. Hoffman JF, Joiner W, Nehrke K, Potapova O, Foye K, Wickrema A. The hSK4 (KCNN4) isoform is the Ca2+-activated K+ channel (Gardos channel) in human red blood cells. Proc Natl Acad Sci U S A. 2003;100(12):7366-71. doi: 10.1073/pnas.1232342100.
52. Sherwood JB, Goldwasser E, Chilcote R, Carmichael LD, Nagel RL. Sickle cell anemia patients have low erythropoietin levels for their degree of anemia. Blood. 1986;67(1):46-9.
53. Pulte D, Nagalla S, Caro J. Erythropoietin levels in patients with sickle cell disease not in vaso-occlusive crisis. Blood. 2012;120(21):3242. doi: 10.1182/blood.V120.21.3242.3242.
54. Little JA, McGowan VR, Kato GJ, Partovi KS, Feld JJ, Maric I, et al. Combination erythropoietin-hydroxyurea therapy in sickle cell disease: experience from the National Institutes of Health and a literature review. Haematologica. 2006;91(8):1076-83.
55. Qasim N, Mahmood R. Diminution of oxidative damage to human erythrocytes and lymphocytes by creatine: possible role of creatine in blood. PLoS One. 2015;10(11):e0141975. doi: 10.1371/journal.pone.0141975.
56. Kabore A, Tamboura HH, Traore A, Meda R, Kiendrebeogo M, Belem AMG, et al. Phytochemical analysis and acute toxicity of two medicinal plants (*Anogeissus leiocarpus* and *Daniellia oliveri*) used in traditional veterinary medicine in Burkina Faso. Arch Appl Sci Res. 2010;2(6):47-52.
57. Olugbami JO, Gbadegesin MA, Odunola OA. In vitro evaluation of the antioxidant potential, phenolic and flavonoid contents of the stem bark ethanol extract of *Anogeissus leiocarpus*. Afr J Med Med Sci. 2014;43(Suppl 1):101-9.
58. Esomonu UG, El-Taalu AB, Anuka JA, Ndodo ND, Salim MA, Atiku MK. Effect of ingestion of ethanol extract of *Garcinia kola* seed on erythrocytes in wistar rats. Niger J Physiol Sci. 2005;20(1-2):30-2.
59. Oluyemi KA, Omotuyi IO, Jimoh OR, Adesanya OA, Saalu CL, Josiah SJ. Erythropoietic and anti-obesity effects of *Garcinia cambogia* (bitter kola) in Wistar rats. Biotechnol Appl Biochem. 2007;46(Pt 1):69-72. doi: 10.1042/ba20060105.
60. Zheng KY, Choi RC, Cheung AW, Guo AJ, Bi CW, Zhu KY, et al. Flavonoids from Radix Astragali induce the expression of erythropoietin in cultured cells: a signaling mediated via the accumulation of hypoxia-inducible factor-1alpha. J Agric Food Chem. 2011;59(5):1697-704. doi: 10.1021/jf104018u.
61. Antwi-Boasiako C, Dankwah GB, Aryee R, Hayfron-Benjamin C, Donkor ES, Campbell AD. Oxidative Profile of Patients with Sickle Cell Disease. Med Sci (Basel). 2019;7(2). doi: 10.3390/medsci7020017.
62. Nku-Ekpang O-A, Ofem O, Oka V, Jaja S. Impact of vitamins C and E supplement on anti-oxidant enzymes (catalase, superoxide dismutase, and glutathione peroxidase) and lipid peroxidation product (malondialdehyde levels) in sickle subjects. Trop J Med Res. 2016;19(2):100-5. doi: 10.4103/1119-0388.185427.
63. Kuo SM. Flavonoids and gene expression in mammalian cells. In: Buslig BS, Manthey JA, eds. Flavonoids in Cell Function Flavonoids in Cell Function. Boston, MA: Springer; 2002. p. 191-200. doi: 10.1007/978-1-4757-5235-9_18.
64. Kuo SM. Flavonoids and gene expression in mammalian cells. Adv Exp Med Biol. 2002;505:191-200. doi: 10.1007/978-1-4757-5235-9_18.
65. Yahfoufi N, Alsadi N, Jambi M, Matar C. The immunomodulatory and anti-inflammatory role of polyphenols. Nutrients. 2018;10(11). doi: 10.3390/nu10111618.
66. Gibbs WN, Wardle J, Serjeant GR. Glucose-6-phosphate dehydrogenase deficiency and homozygous sickle cell disease in Jamaica. Br J Haematol. 1980;45(1):73-80. doi: 10.1111/j.1365-2141.1980.tb03812.x.
67. Steinberg MH, West MS, Gallagher D, Mentzer W. Effects of glucose-6-phosphate dehydrogenase deficiency upon sickle cell anemia. Blood. 1988;71(3):748-52.
68. Smits HL, Oski FA, Brody JI. The hemolytic crisis of sickle cell disease: the role of glucose-6-phosphate dehydrogenase deficiency. J Pediatr. 1969;74(4):544-51. doi: 10.1016/s0022-3476(69)80037-5.
69. Konotey-Ahulu FI. Glucose-6-phosphate dehydrogenase deficiency and sickle-cell anemia. N Engl J Med. 1972;287(17):887-8. doi: 10.1056/nejm197210262871719.
70. Lewis RA, Kay RW, Hathorn M. Sickle cell disease and glucose-6-phosphate dehydrogenase. Acta Haematol. 1966;36(5):399-411. doi: 10.1159/000209420.
71. Piomelli S, Reindorf CA, Arzanian MT, Corash LM. Clinical and biochemical interactions of glucose-6-phosphate dehydrogenase deficiency and sickle-cell anemia. N Engl J Med. 1972;287(5):213-7. doi: 10.1056/nejm197208032870502.
72. Malumbres M, Barbacid M. Mammalian cyclin-dependent kinases. Trends Biochem Sci. 2005;30(11):630-41. doi: 10.1016/j.tibs.2005.09.005.
73. Malumbres M. Cyclin-dependent kinases. Genome Biol. 2014;15(6):122. doi: 10.1186/gb4184.
74. Sasaki Y, Jensen CT, Karlsson S, Jacobsen SE. Enforced expression of cyclin D2 enhances the proliferative potential of myeloid progenitors, accelerates in vivo myeloid reconstitution, and promotes rescue of mice from lethal myeloablation. Blood. 2004;104(4):986-92. doi: 10.1182/blood-2003-07-2277.
75. Lam EW, Glassford J, Banerji L, Thomas NS, Sicinski P, Klaus GG. Cyclin D3 compensates for loss of cyclin D2 in mouse B-lymphocytes activated via the antigen receptor and CD40. J Biol Chem. 2000;275(5):3479-84. doi: 10.1074/jbc.275.5.3479.
76. Solvason N, Wu WW, Parry D, Mahony D, Lam EW, Glassford J, et al. Cyclin D2 is essential for BCR-mediated proliferation and CD5 B cell development. Int Immunol. 2000;12(5):631-8. doi: 10.1093/intimm/12.5.631.
77. Sorrentino BP. Clinical strategies for expansion of haematopoietic stem cells. Nat Rev Immunol. 2004;4(11):878-88. doi: 10.1038/nri1487.
78. Karimian A, Ahmadi Y, Yousefi B. Multiple functions of p21 in cell cycle, apoptosis and transcriptional regulation after DNA damage. DNA Repair (Amst). 2016;42:63-71. doi: 10.1016/j.dnarep.2016.04.008.
79. Pagadala NS, Syed K, Tuszynski J. Software for molecular docking: a review. Biophys Rev. 2017;9(2):91-102. doi: 10.1007/s12551-016-0247-1.
80. Ashwini S, Varkey SP, Shantaram M. In Silico docking of polyphenolic compounds against Caspase 3-HeLa cell line protein. Int J Drug Dev Res. 2017;9:28-32.
81. Codorniu-Hernández E, Rolo-Naranjo A, Montero-Cabrera LA. Theoretical affinity order among flavonoids and amino acid residues: An approach to understand flavonoid–protein interactions. J Mol Struct. 2007;819(1-3):121-9. doi: 10.1016/j.theochem.2007.05.036.
82. Panche AN, Diwan AD, Chandra SR. Flavonoids: an overview. J Nutr Sci. 2016;5:e47. doi: 10.1017/jns.2016.41.
83. Lipinski CA, Lombardo F, Dominy BW, Feeney PJ. Experimental and computational approaches to estimate solubility and permeability in drug discovery and development settings. Adv Drug Deliv Rev. 2001;46(1-3):3-26. doi: 10.1016/s0169-409x(00)00129-0.
84. Jorgensen WL. Efficient drug lead discovery and optimization. Acc Chem Res. 2009;42(6):724-33. doi: 10.1021/ar800236t.
85. Agati G, Tattini M. Multiple functional roles of flavonoids in photoprotection. New Phytol. 2010;186(4):786-93. doi: 10.1111/j.1469-8137.2010.03269.x.
86. Humphrey W, Dalke A, Schulten K. VMD: visual molecular dynamics. J Mol Graph. 1996;14(1):33-8, 27-8. doi: 10.1016/0263-7855(96)00018-5.